Heat flux control by means of tangential air injection at high supersonic speeds.

Borovoy V.Ya.[1], Vasilevskiy E.B.[1], Egorov I.V.[1,2], Mosharov V.E.[1], Radchenko V.N.[1], Chuvakhov P.V.[1,2], Shtapov V.V.[1]

[1] Central Aerohydrodynamic Institute (TsAGI)
1 Zhukovskogo str., Zhukovsky, Moscow reg., Russia, 140180

[2] Moscow Institute of Physics and Technology State University (MIPT)
9 Institutskiy pereulok, Dolgoprudny, Moscow reg., Russia, 141700

Abstract

Results of experimental and numerical investigation of heat flux control over a sharp cone surface by means of tangential air blowing of cooling gas (air) through continuous circular slot at cone surface are presented. Flow structure in the slot vicinity is analysed. Local cooling effect is found to rise as total pressure of coolant increases. However one needs to find an optimal state between cooling and total mechanical energy losses due to coolant / outer flow interaction.

1. Introduction

Gas slowed down near streamed surface is heated strongly at high supersonic speeds, and excessive thermal loads emerge to the surface, which can lead to its being overheated and finally destructed. In order to prevent damage of this type heat protection systems are used. Passive ones appear to be simple in use, e.g. ablating covers that absorb a considerable part of thermal energy to destruct themselves. However it is sometimes of practical importance to preserve original shape of a surface to provide a room for its multiple usage. Active heat protection such as effusion / film cooling (here and after it is simply referred to as film cooling) is an urgent problem in these cases. This technique of injecting a layer of a cold gas near the surface is realized via various slot devises and has been put in practice for a long time. For example, active heat protection has been applied to practical problems of cooling turbine blades [1], combustor liners [2] and rocket nozzles [3], although this method is not in use for heat protection of outer surfaces of flying vehicles.

Film cooling approach has been investigated earlier both experimentally and numerically fot different problem configurations. For instance, experimental studies of tangential slot injection at Mach 6 [4, 5] shows that the film cooling in two-dimensional high speed turbulent flow is significantly more effective then indicated by simple extrapolations of low speed results to high speeds. The same problem configuration is considered in three-dimensional case [6] where coolant is supplied by a tangential step slot at some sweep angle to the outer stream propagation. It is found that cooling effectiveness is not significantly affected by sweeping the slot. [7] presents heat-transfer results which indicate the effect of divergence on film cooling on a cone at angle of attack. In [8] reduction in drag due to friction is obtained for M = 6 flow by direct measurements in case of coolant injection in downstream direction through both a single and multiple flush slots at small inclination angle to the surface. It is noted as well that tangential injection through a step slot appears to be more effective in friction drag (and consequently heat flux) reduction.

In [9] hypersonic flow over a flat plate with blunt leading edge is considered. Layer of cold gas is supplied by a step slot located at the bluntness region. It has been shown that it is possible to protect a region of the stagnation point by tangential injection in upstream direction, with coolant layer travelling along the surface without separation.

The technique of film cooling at supersonic speeds is investigated extensively nowadays. For example, in [10,11,12,13] results of numerical parametric studies of the influence of governing parameters (Reynolds number, Mach number, wall temperature) and injection setup effects (hole spacing, blowing ratio, etc.) on cooling efficiency are presented for laminar boundary layer; [14] deals with turbulent boundary layer; [15, 16, 17] give results of similar experimental investigations for different states of boundary layer.

Unfortunately most of works devoted to film cooling problems consider internal flow problems while there are not enough data for external ones. In this work feasibility of film cooling heat flux control over a sharp cone is investigated experimentally and numerically. The coolant is supplied via a continuous circular slot at supersonic speed into a laminar boundary layer. This problem relates to some kind of supersonic inlets, what will be discussed further.

2. Experimental setup

1.2 Wind tunnel UT – 1M

The experiments have been conducted in wind tunnel UT – 1M facilities. The scheme of the tunnel is presented in figure 1. This is a shock wind tunnel operating in Ludwig scheme. Working gas is supplied to high pressure duct of *12 m length* and *70 mm diameter*. An electrical heater located inside the duct provides gas heating up to a given temperature. At the end of the duct sequentially placed are two diaphragms (3), a nozzle (4), a *0.5 m diameter* test section (5) with optical windows (6), an exhaust chamber (7) with an expansion tank. After the diaphragm opening, an expansion wave propagates along the duct, reflects from the opposite wall and returns back to the nozzle, which takes approximately *40 msec*. All flow parameters remain constant during this time. One can find a more detailed description of the wind tunnel UT – 1M in [18].
Profiled *Mach 5* nozzle *500 mm* in diameter was used in all experiments. Gas was heated to $T_0 = 700\ K$ and pressurized to $p_0 = 50\ bar$ before any run.

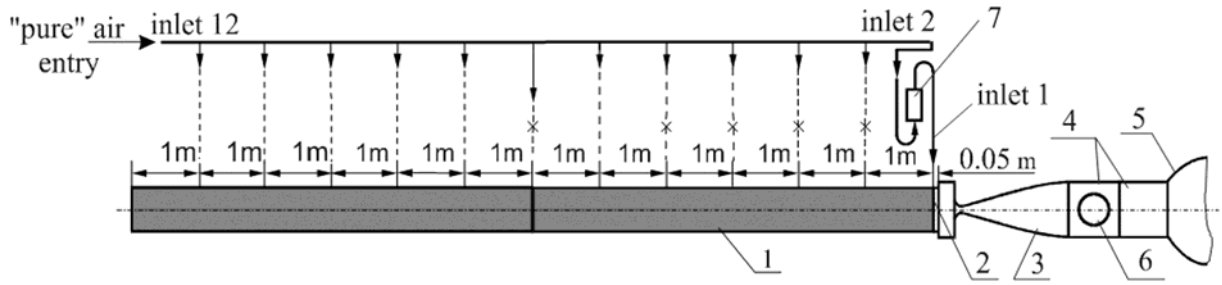

Figure 1: Wind tunnel UT – 1M scheme. 1 — duct, 2 — diaphragm, 3 — nozzle, 4 — test section, 5 — exhaust chamber, 6 — optical window, 7 — mixing device

2.2 The model

The model under consideration is a sharp cone (bluntness radius less then 0.01 mm) with half-angle 8° and $L = 400\ mm$ length along its axis (figure 2). Leading edge of a slot is located at *68.9 mm* and trailing one at *71.15 mm* apart from the cone nose. Inclination angle of the slot is $\alpha_j = 10^\circ$ with respect to the cone forming line. A longitudinal section of the slot is the diverging cone with 6° half-angle and minimal height of $\delta^* = 0.3\ mm$ at slot inlet. The entire surface is manufactured of thermoinsulating material AG – 4, except some low-sized elements which are made from steel, e.g.: cone nose, small rounding of slot surfaces. The use of thermoinsulating materials makes it possible to apply the Thermal Sensitive Paint (TSP) technique for measuring surface heat fluxes. A scheme of the slot and its geometry is shown in figure 3.

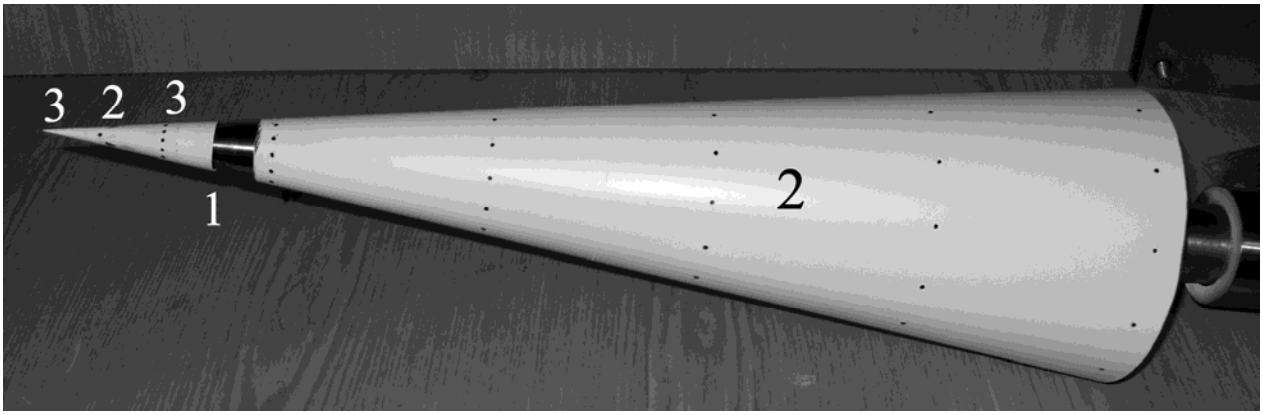

Figure 2: Model. 1 — slot leading edge, 2 — termoinsulating material, 3 — steel

All runs have been carried out at zero angle of attack. Injection is performed by a fast-operating coolant supply unit shown in figure 4. Its principal parts are: a 40 l vessel (16), a supply valve (14) for filling the tank, a discharge valve

(13), a fast-operating valve (8) with big pass section enabling usage of high pressure gas, a fast-operating pneumatic electrical valve (9) for governing the valve (8).

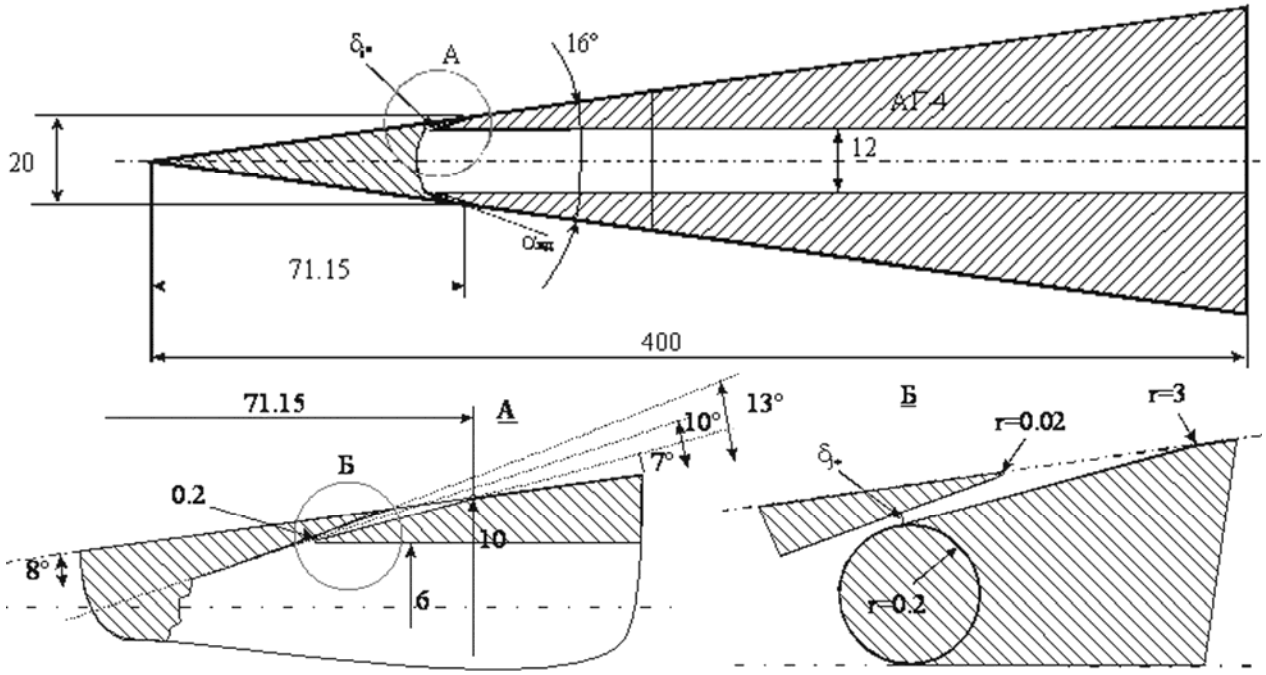

Figure 3: Model scheme

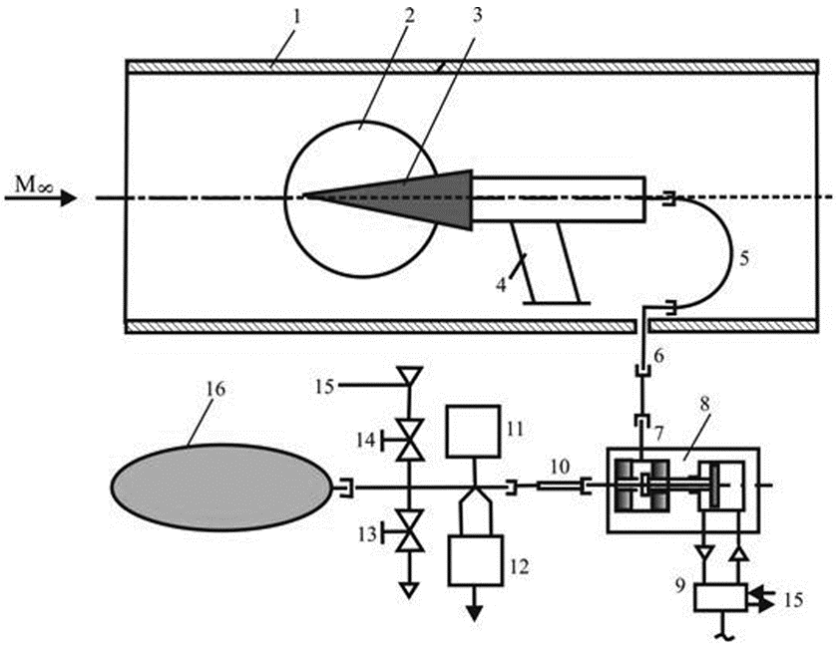

Figure 4: Coolant supply scheme. 1 — working chamber wall, 2 — optical window, 3 — model, 4 — model holder, 5 – 7, 10 — coolant supply pipes, 8 — main air valve, 9 — governing electrical valve, 11 — manometer, 12 — temperature sensor, 13, 14 — supply and discharge valves, 15 — high-pressure line, 16 — vessel

The pass section of any part of the fast-operating supply unit is greater then *100 mm*^{2}, which is much grater then the similar property of the slot critical section $f_* = 12.34\ mm^2$; therefore the speed of cooling gas in the unit channels before the critical section has been considerably less then the speed of sound. Hydraulic experiments of the unit incorporated into the model have shown that hydraulic drag of the supply unit is negligible compared with that of the model. Operation of the valve (9) was synchronized with wind tunnel behavior and its measuring system. Eventually, steady flow regime inside the model sets in *0.02 msec*. Figure 5 illustrates the dependence of coolant mass flow rate versus vessel pressure.

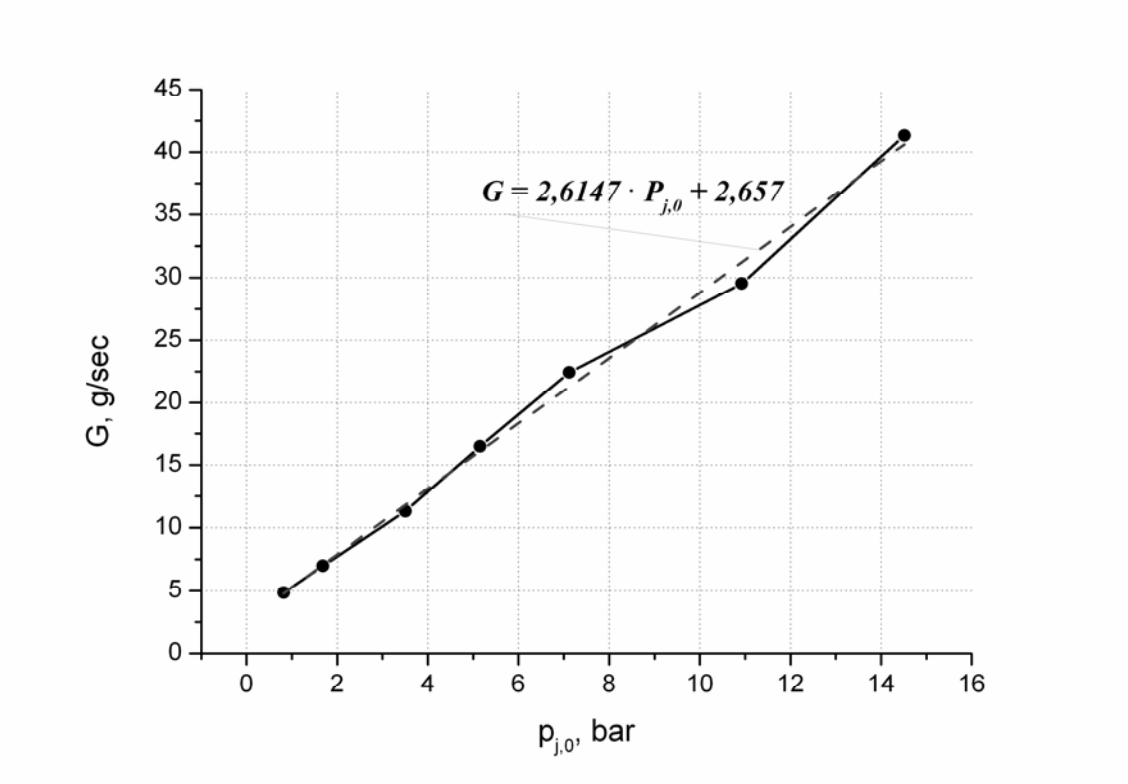

Figure 5: Mass rate of injected gas versus vessel pressure (total pressure of coolant)

2.3 Experimental methodology

The cone model is installed inside the tunnel test section along stream axis with zero angle of attack. Shooting of flow pattern around the model is performed by two cameras with high temporal resolution of *500 fps*. Visualization of the flow is carried out by Schlieren method.
Thermal Sensitive Paint method (TSP) is used in order to gain information on heat fluxes over the entire streamed surface. This method is based on the temperature quenching of luminescence of organic paint. The heat flux at any visible point of streamed surface is derived based on the temperature increment value measured for a given time interval. Detailed information on TSP method in wind tunnel of Ludwig scheme can be found in [19, 20].

3. Numerical problem formulation

3.1 Numerical method

Numerical part of the investigation has been performed on the base of Ansys Fluent software. A flow of viscous perfect gas with constant Prandtl number is considered in the frame of unsteady RANS equations. Molecular viscosity is calculated according Sutherland's formula.
Two turbulent models are considered as RANS closures. These are: standart k-ω model and its modification k-ω transitionSST model. The former is used downstream the slot leading edge while the upstream region is supposed to be laminar. The later is aimed at making a border between laminar and turbulent region unfixed. Both closures give the same results for the problem configuration in hand. Therefore we are considering those of k-ω transitionSST model only. Using of this turbulence closure is important for example in case of considering a problem of coolant injection in direction normal to the surface when it is possible for separation region to arise upstream the slot position. It is here that one has to realize whether the flow is laminar or turbulent downstream the separation point. This ambiguity can be eliminated using respective experimental data.
Density-based implicit coupled solver with second order approximation in space and time is used. Roe method is used to approximate convective part of numerical fluxes.

3.1 Calculating region, grid, initial and boundary conditions

Flow modeling around the solid cone (total nods count ~415000) and the cone with the slot device (total nods count ~500000) have been performed. Computational grid lines are clustered near the cone surface so that a boundary layer close to the slot leading edge turns out to be resolved with ~100 grid lines. A turbulent boundary layer exists downstream the slot. Its resolution was good as well, with ~10 grid lines being inside a laminar sublayer.
No-slip conditions *(u = 0, v = 0)* are imposed onto the boundary corresponding to the cone surface that is considered to be isothermal ($T_w = 288\ K$). This conforms to the wind tunnel UT – 1M experiments where a run time interval is short enough for the model to be heated strongly. The temperature rise of the model surface for an experiment is approximately *5 K*.
Far field conditions were imposed onto the outer boundary of a calculation region:

$$\begin{aligned} p_\infty &= p_0 \times \left(1 + 0.5(\gamma - 1)\mathrm{M}_\infty^2\right)^{-\gamma/(\gamma-1)}, \\ T_\infty &= T_0 \times \left(1 + 0.5(\gamma - 1)\mathrm{M}_\infty^2\right)^{-1}, \\ p_0 &= 50\,bar, T_0 = 700\,K, \mathrm{M}_\infty = 5, \gamma = 1.4. \end{aligned} \tag{1}$$

Here T_0, p_0, M_∞, γ are stagnation temperature, total pressure, free stream Mach number, and specific heat ratio consequently. Symbol ∞ relates to free stream values. These parameters give the appropriate unit length Reynolds number $Re_{\infty,1} = 3.85 \times 10^7\ m^{-1}$.
Flow inlet condition is set on the slot inlet. Air is considered as cooling gas. Its stagnation temperature is $T_{j,0} = T_w = 288\ K$ and total pressure varies among $p_{j,0} = 1, 2, 4, 8\ bar$, in accordance with experiments.
Results of calculations on a coarse grid are interpolated onto the fine grids and then used as initial estimations for the numerical problem involved.

4. Results and analysis

4.1 Flow visualization

Shadow patterns of entire flow field near the model are obtained for different coolant mass flows (figure 6). A shock arises from the nose of the sharp cone without the slot device in supersonic flow. In case of slot injection, a shock next to the slot trailing edge is visible. It is due to reattachment of the flow separated at the slot leading edge. Flow structure in the slot region is complicated enough because of interaction of two streams: outer gas and cooling gas. Dividing line and mixing layer emerge. It is not possible to distinguish all the features of flows interaction in details. Numerical simulation will address them further. However shock in outer flow originating at slot due to the interaction is visible. Moreover an inclination angle of this shock increases with respect to the model axis as the coolant mass rate enlarges.

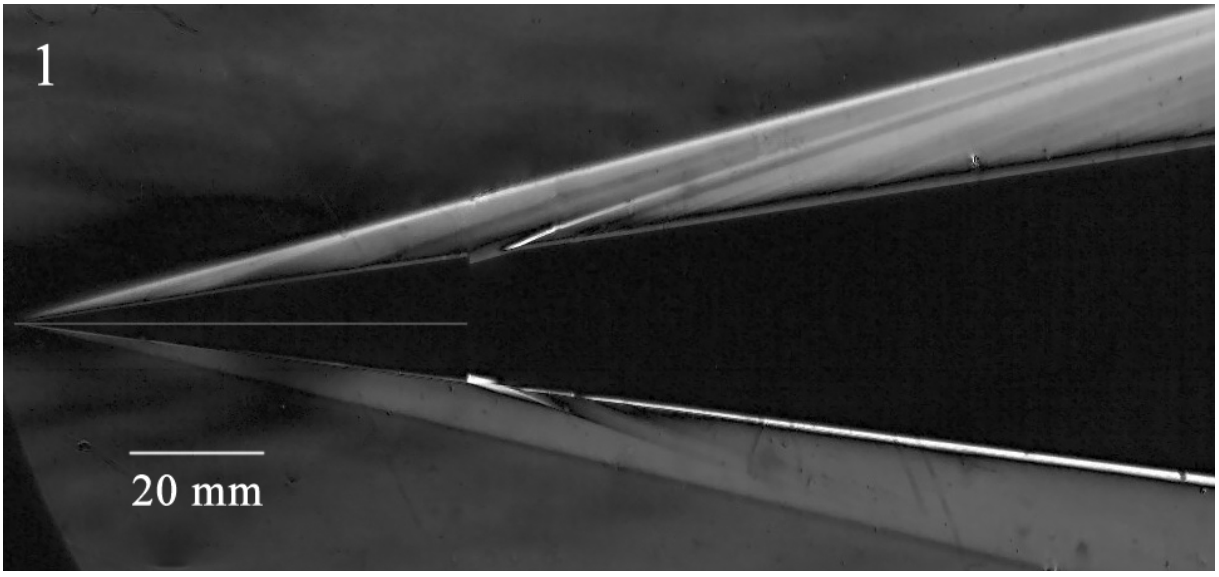

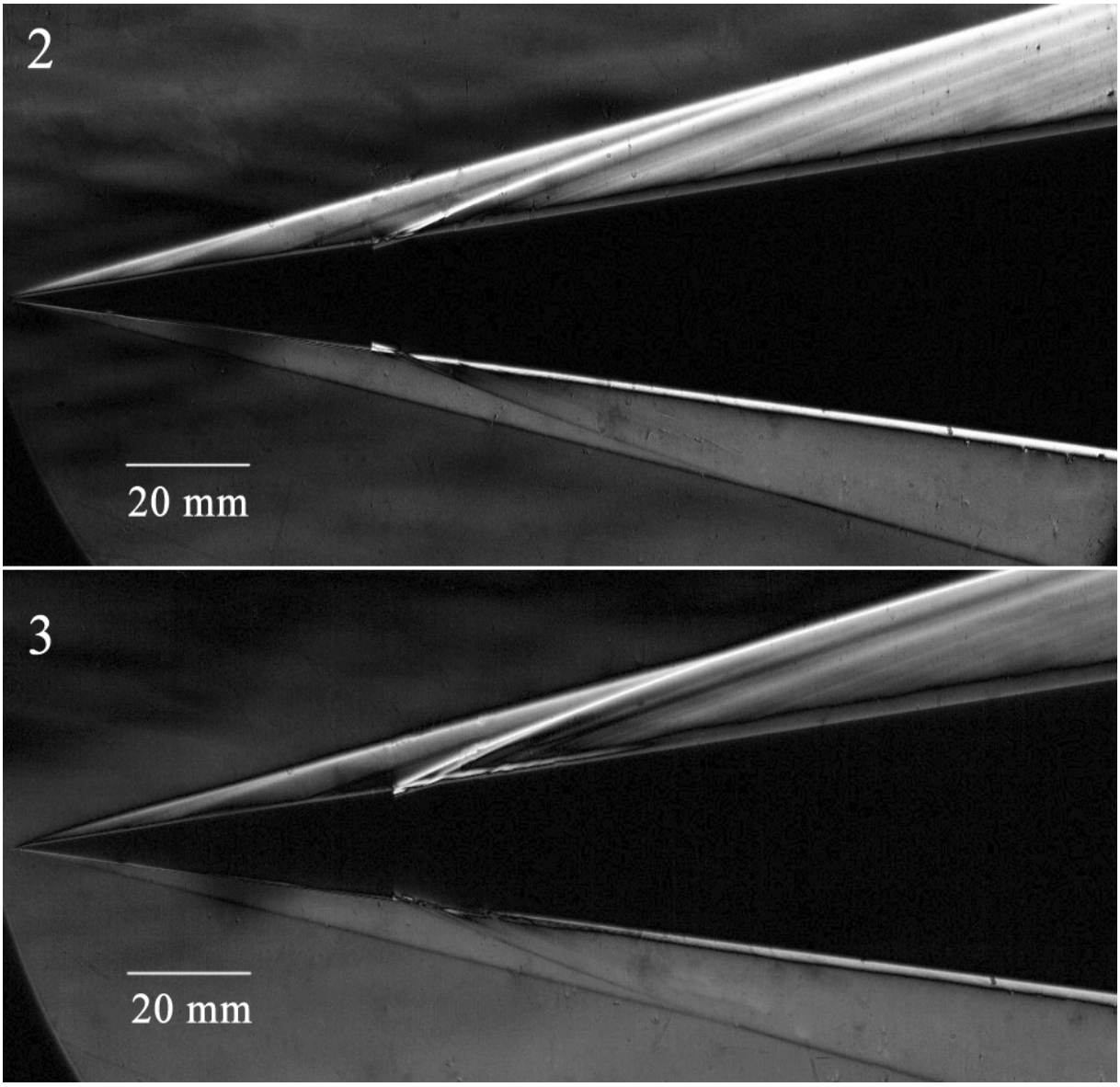

Figure 6: Shadow patterns. 1 — slot without injection, 2 — $p_{j,0} = 2$ *bar*, 3 — $p_{j,0} = 8$ *bar*

4.2 Slot flow scheme

Figure 7 illustrates an example of a numerical simulation (pressure field) near the slot and appropriate flow scheme. Interaction of two streams of viscous gas at different pressures and velocities results in forming a complicated flow pattern with shock in outer flow and shock in coolant gas. The later falls onto the slot trailing edge to form a separation bubble that in turn gives rise to a third shock of reattachment.

4.3 Angle of inclination of shock in outer flow

Increasing the total pressure of injected gas an effective “obstacle” for outer flow to overcome enlarges. This leads to rising of its inclination angle and intensity of the shock in outer flow. Comparison of calculated and experimental results for angles of inclination of the first shock is given by figure 8. Some discrepancy may be due to the error in angle measuring approach.

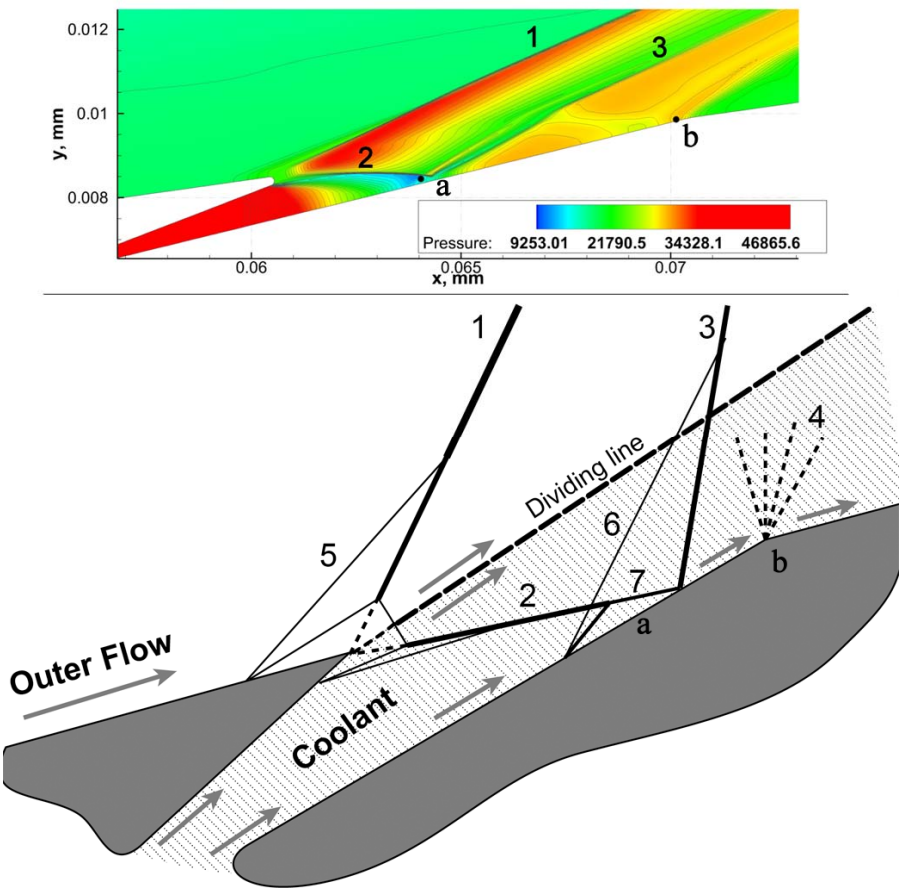

Figure 7: Top — calculated pressure field, $p_{j,0} = 8$ *bar*; bottom — slot flow scheme
1 — shock 1, 2 — shock 2, 3 — shock 3, 4 — rarefication fan, 5 — separation shock 1, 6 — separation shock 2, 7 — separation because of shock 2; a, b — reference points

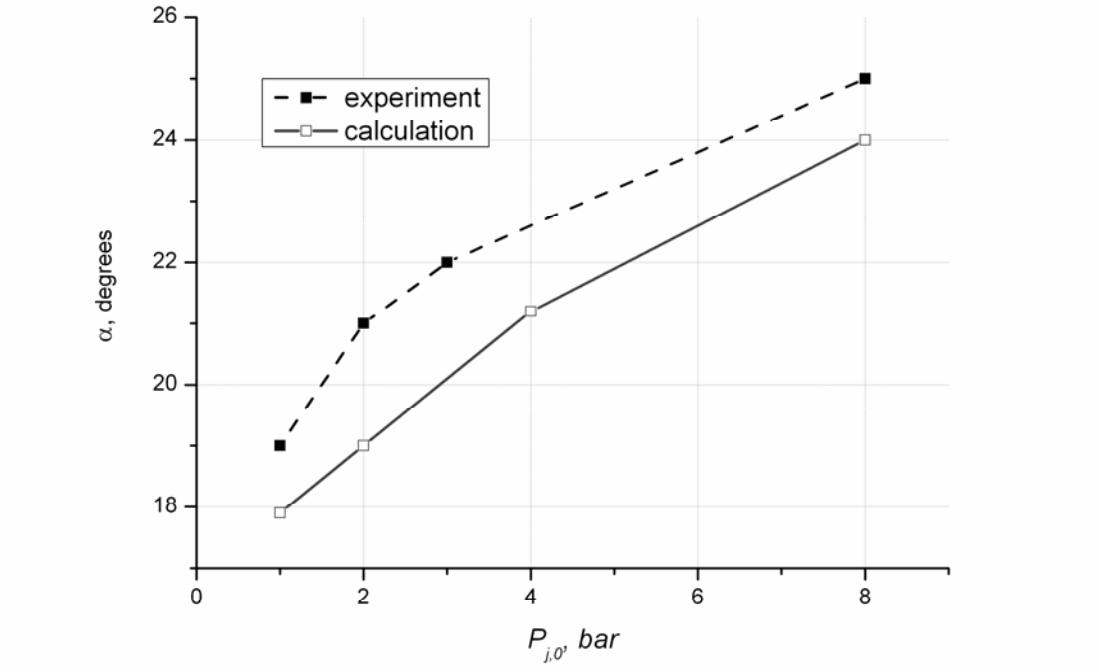

Figure 8: Shock 1 inclination

4.4 Streamlines in the slot vicinity

Figure 9 illustrates the calculated patterns of Mach number and streamlines including the dividing line. Separation regions near the slot are conspicuous. The coolant is injected at supersonic speeds in any case considered. The thickness of cooling gas layer downstream the slot increases as coolant total pressure increases, which indirectly indicates the coolant mass rate growth.
Thickness of this layer and its coolant Mach number can be estimated if motion of gas inside the slot device is supposed to be isentropic. Having neglected the total pressure losses due to friction and shocks, one can derive:

$$\frac{A_{out}}{A^*} = \frac{2\pi r_{out} h_{out}}{2\pi r^* h^*} = \left(\frac{2}{\gamma-1}\right)^{\frac{\gamma+1}{2(\gamma-1)}} \left(\frac{\gamma-1}{2}\right)^{1/2} \frac{\kappa^{\frac{\gamma+1}{2(\gamma-1)}}}{\left(\kappa^{\frac{\gamma-1}{\gamma}}-1\right)^{1/2}}, \qquad (2)$$

where A_{out} and A^* are sections of coolant stream on the slot exit and in the slot critical section respectively, r and h are its appropriate radius and thickness; $\kappa = p_{0,j} / \hat{p}$, $\hat{p}$ is static pressure coolant expands to (given by calculation).

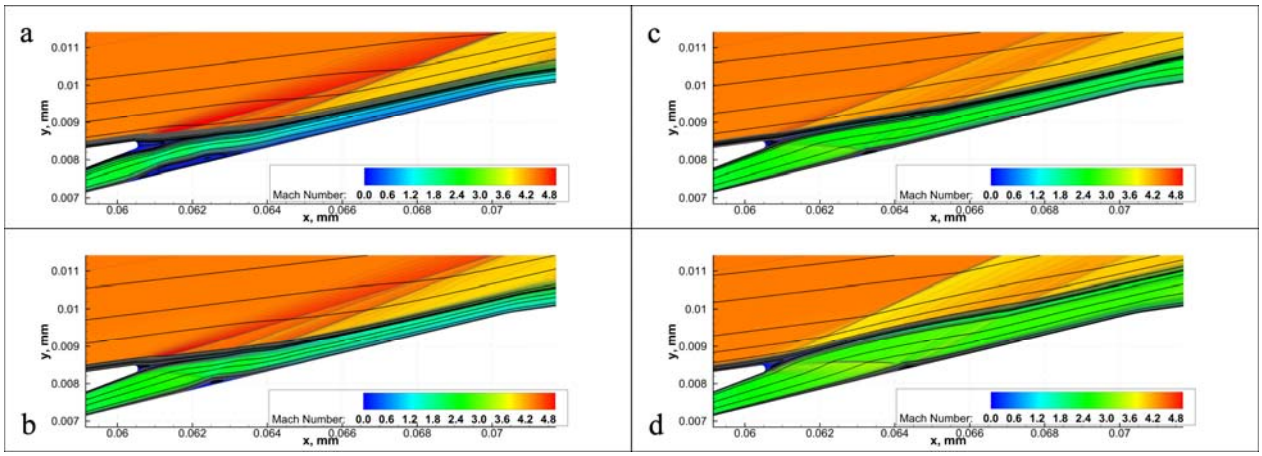

Figure 9: Calculated Mach number field and streamlines in slot vicinity (dividing line is bold)
a — $p_{j,0} = 1$ *bar*, b — $p_{j,0} = 2$ *bar*, c — $p_{j,0} = 4$ *bar*, d — $p_{j,0} = 8$ *bar*

In the case of $p_{0,j} = 8$ bar we have $\hat{p} \sim 2\times10^4$ *Pa* and $h_{out} \sim 4.5 h^* r^* / r_{out} = 0.9\,mm$. At the same time the calculated value of h_{out} given by temperature profile is equal to ~*1 mm*, what is close to the estimation.
Based on Mach number distribution one can conclude that different flow schemes can be realized:

1. expansion with acceleration of the outer flow along with deceleration of injected gas stream to $M < 1$, with forming a shock in coolant and separation bubble at back wall of the slot device;
2. compression of the outer flow due to a weak shock without separation and nearly constant coolant flow speed.

Pendent shock (third shock) is formed in both cases because of interaction of inner shock (shock 2) with the slot device.

4.5 Surface cooling scheme

Let us consider a similar problem of outer flow / coolant interaction in case of flat plate with a tangential step-slot (figure 10). Mixing layer begins to develop from the slot leading edge; its boundaries in outer flow and coolant stream are inclined at different angles with respect to a dividing line. Until the later boundary reaches the plate, cooling efficiency should be maximal and constant because the coolant recovery temperature is nearly invariable.
This temperature turns out to be less then T_w due to $T_{0,j} = T_w$. That is why negative heat flux (from wall to gas) will be observed over the zone described (here and after we will refer to this zone as effectively cooled zone). The experimentally and numerically obtained values of the length of this zone agree with each other, as can be seen further.

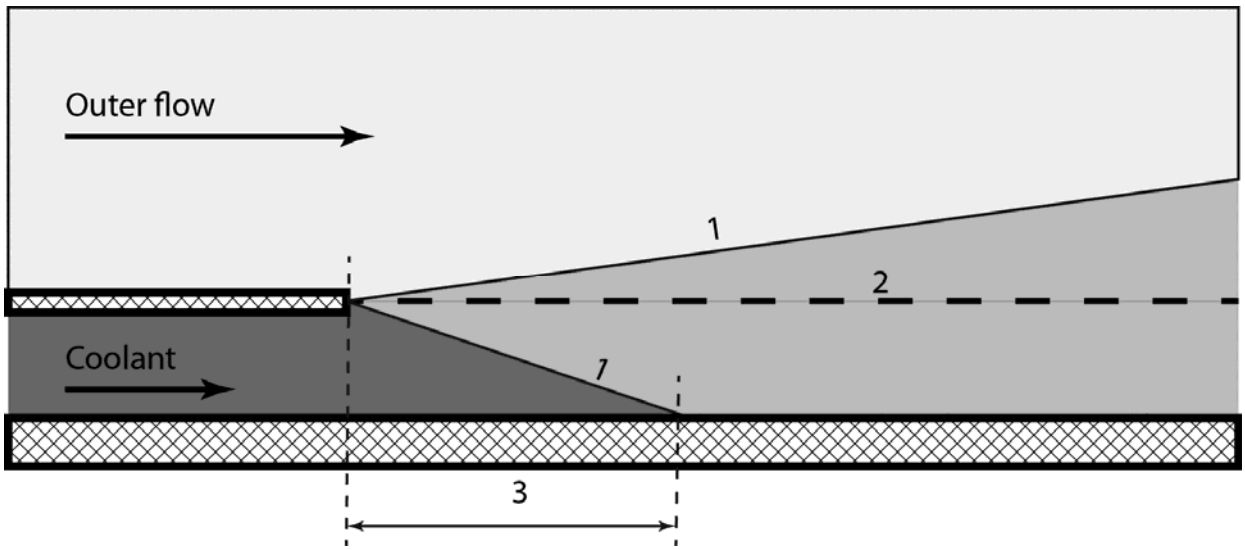

Figure 10: Flat plate film cooling scheme. 1 — mixing layer boundaries, 2 — dividing line, 3 — effectively cooled zone

4.6 Surface heat flux

Figure 11 illustrates experimental data distribution for dimensionless heat flux over the cone generatrix $(St = q / (\rho_\infty V_\infty c_p(T_0 - T_\infty))$ versus dimensionless coordinate x/L, where L is a generatrix total length. In calculations a cone with dimensionless length 0.6 is considered for the sake of simplicity, but the length scale remains the same $(L = 400\ mm)$ in order to compare results. Appropriate calculated dependencies are shown in figure 12.

Both experimental and calculation results indicate an increase in length of effectively cooled zone as coolant total pressure (and consequently coolant mass rate) rises. Both approaches also show negative heat fluxes over this zone where the wall heats the gas. This occurs due to two reasons: firstly because injected gas has not been mixed with outer flow yet and its stagnation temperature is equal to wall temperature; secondly, coolant recovery temperature is less the stagnation one because the Prandtl number for air is less then one.

Comparison of calculation and experimental results for the case of $p_{j.0} = 8\ bar$ with known self-similar solutions, empirical data, and numerical data gained on the base of TsAGI inhouse software *HSFlow* [21], is presented in figure 13.

Calculations by Fluent software give correct results for heat fluxes over the laminar region (upstream the slot) compared with the self-similar solution profiles and the empirical data, but for turbulent region (downstream the slot) they turn out to be slightly underestimated. Experimental data over the entire surface of the cone are underestimated approximately by the factor of 1.5 when compared with Fluent results. A simple estimate shows that this discrepancy can take place in case of gas in the duct of wind tunnel being underheated, that is its stagnation temperature was approximately $600\ K$ instead of $700\ K$. It is the discrepancy that has been observed for all the experiments done. Despite this fact, however, the qualitative behavior of heat flux dependencies, the coolant layer thickness and the effectively cooled zone length are modeled identically both in experiments and calculations.

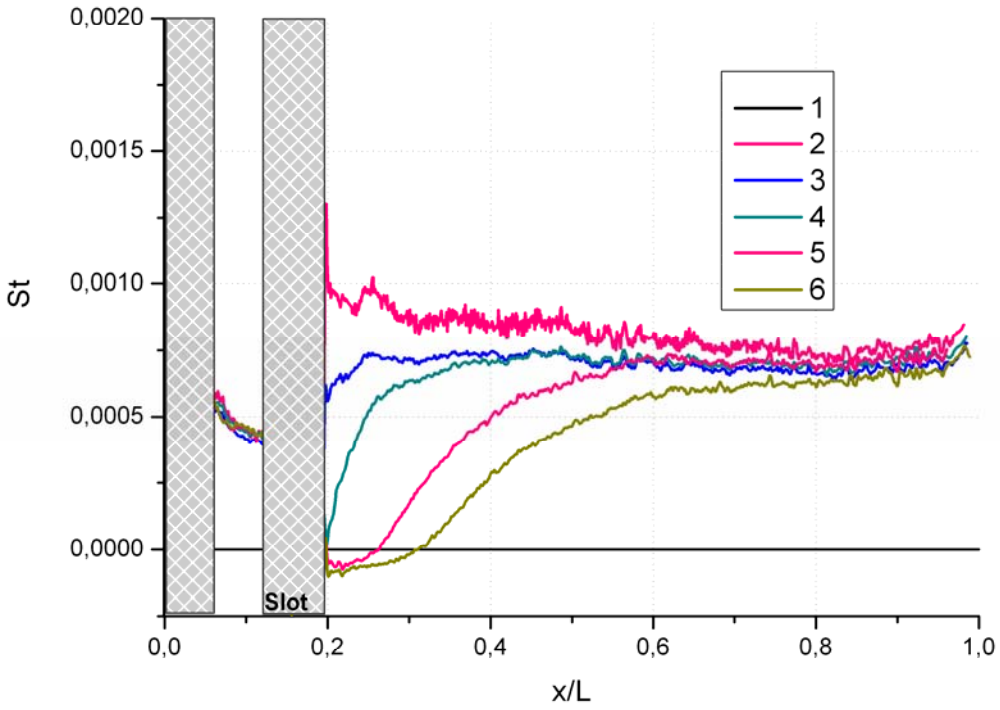

Figure 11: Stanton number over cone generatrix, experiment. 1 — slot without injection, 2 — $p_{j,0}$ = *1 bar*, 3 — $p_{j,0}$ = *2 bar*, 4 — $p_{j,0}$ = *4 bar*, 5 — $p_{j,0}$ = *8 bar*, 6 — $p_{j,0}$ = *16 bar*

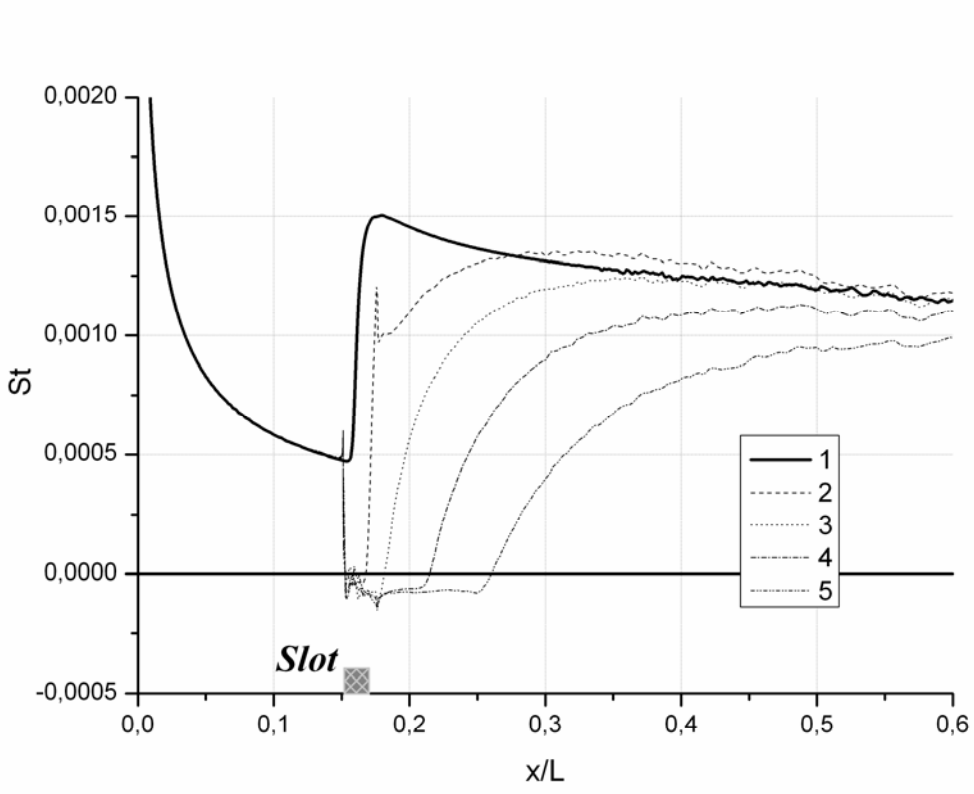

Figure 12: Stanton number over cone generatrix, calculations. 1 — solid cone, 2 — $pj_{,0}$ = *1 bar*, 3 — $p_{j,0}$ = *2 bar*, 4 — $p_{j,0}$ = *4 bar*, 5 — $p_{j,0}$ = *8 bar*

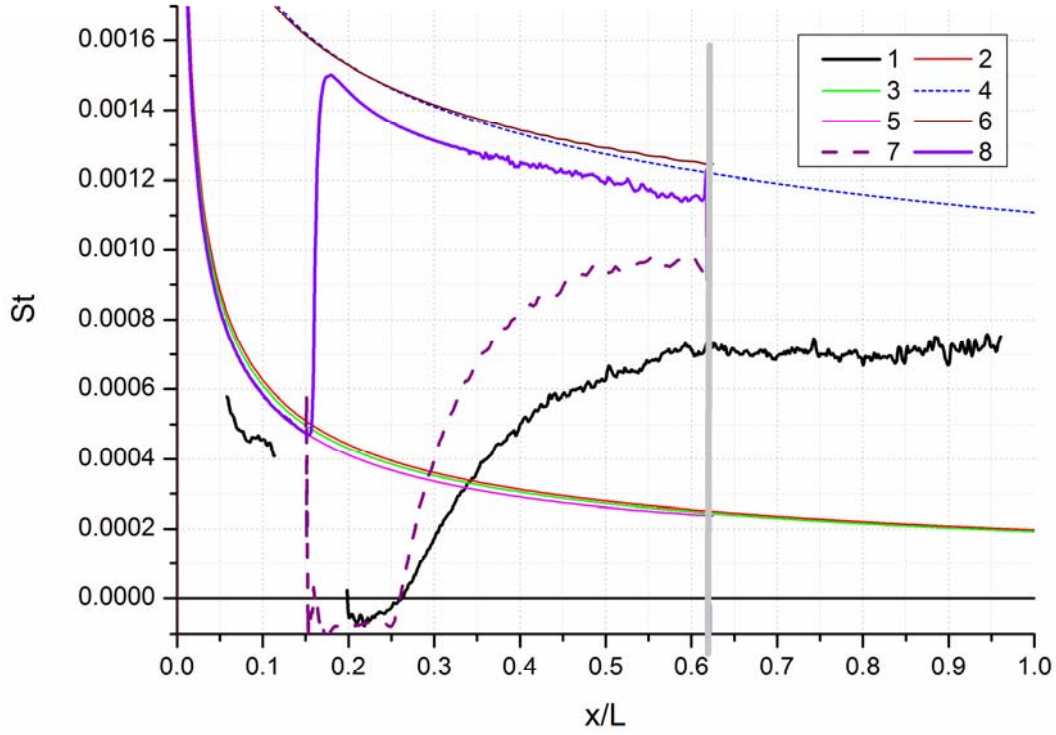

Figure 13: Verification. 1 — experiment $p_{j,0} = 8$ *bar*, 2 — self-similar laminar solution [22], 3 — laminar [23], 4 — turbulent [23], 5 — solid cone *HSFlow* (inhouse CFD code [21]) laminar calculation, 6 — solid cone *HSFlow* turbulent calculation, 7 — Fluent $k - \omega$ *transitionSST* $p_{j,0} = 8$ *bar*, 8 — solid cone (Fluent, forced transition at slot position)

4.7 Imaginary air inlet and total pressure losses

Let us consider a cone as an initial part of an air inlet entrance. Let us also consider the inlet to work at design conditions in the absence of slot device, i.e. the shock from the cone nose falls to a shell ring exactly (figure 14).

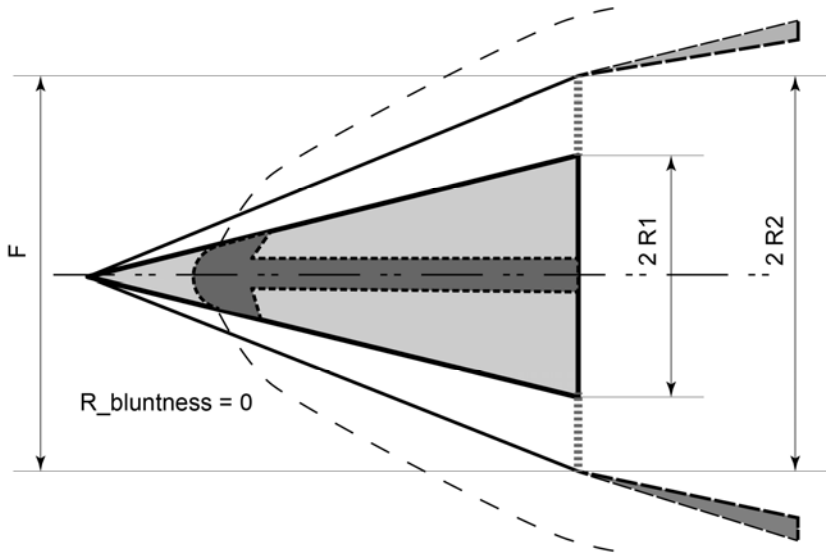

Figure 14: Imaginary inlet scheme

Disturbances in the main stream due to the coolant injection result in change of mass rate and total pressure of gas in a section fixed on the cone surface – entrance section (bold gray dots in figure 14). It is possible to evaluate mass rate and average total pressure across that section based on calculation results and then compare them with the same values in case of free stream parameters:

$$G_{rel} = \frac{G}{G_\infty} = \left(\int_{R_1}^{R_2} \rho u \times 2\pi r dr \right) \Big/ \left(\rho_\infty u_\infty \times F \right) \tag{3}$$

$$p_{0,rel} = \frac{\overline{p}_0}{p_{0,\infty}} = \left[\pi \left(R_2^2 - R_1^2 \right) \right]^{-1} \left(\int_{R_1}^{R_2} p_0 \times 2\pi r dr \right) \Big/ p_{0,\infty} \tag{4}$$

Plots of G_{rel} and $p_{0,rel}$ versus coolant total pressure $p_{j,0}$ are shown in figure 15. It is to be noted that the losses of total pressure and mass rate at the entrance of the imaginary inlet rise with the increase of $p_{j,0}$, which is due to intensifying the impact of the coolant on the outer flow. The losses of this kind would lead to drop in thrust. That is why it is of practical importance to find the optimum state between cooling efficiency and mechanical energy losses due to coolant / outer flow interaction.

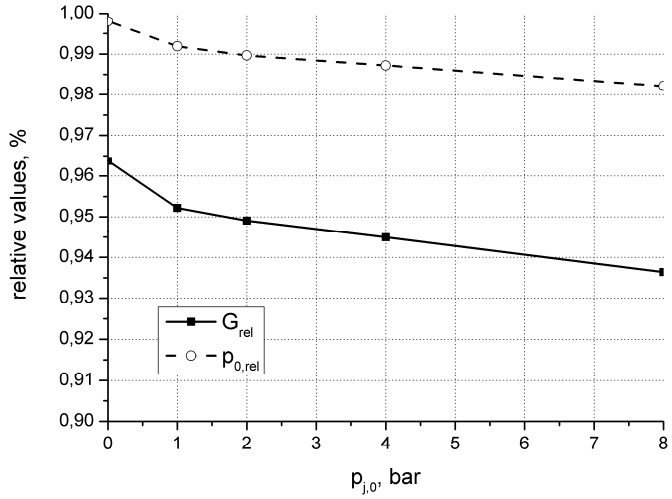

Figure 15: Dependencies of relative mass rate and average total pressure on coolant total pressure $p_{j,0}$

5. Conclusions

1. Experimental and numerical investigation of heat flux control over a cone surface in supersonic air flow by means of tangential cold air injection is carried out.
2. Injection in the slot downstream direction through a continuous circle tiny slot results in local effect of intensive cooling of the surface over a distance of $10...15 \times l_{slot}$, where l_{slot} is a linear size of slot exit along the cone generatrix; cooling effectiveness decreases away from the slot.
3. Calculation results describe the general flow structure correctly from qualitative point of view, and in satisfactory quantitative agreement with experimental data.
4. An increase of total pressure of coolant and consequently its mass rate leads to rise in mechanical energy losses; therefore it is important to find an optimum state between cooling efficiency and the acceptable losses for the applying film cooling approach by tangential air injection.

6. Acknowledgements

This work is supported by the Russian government under grant «Measures to Attract Leading Scientists to Russian Educational Institutions» *(contract No. 11.G34.31.0072).*

References

[1] C. Liess. 1973. Film cooling with injection from a row of inclined circular holes - an experimental study for the application to gas turbine blades. *Von Karman Institute for Fluid Dynamics, Technical note 97.*

[2] D.E. Metzger, R.T. Baltzer, D.I. Takeuchi, P.A. Kuenstler.1972. Heat transfer to film-cooled combustion chamber liners. *ASME Paper No. 72-WA/HT-32*

[3] J.J. Williams, W.H. Geidt. 1970. The effect of gaseous film cooling on the recovery temperature distribution in rocket nozzles. *ASME Paper No. 70-HT/SpT-42*.

[4] K. Parthasarathy, V. Zakkay. 1970. An experimental investigation of turbulent slot injection at mach 6. *AIAA Journal, Vol. 8, No. 7. Pp. 1302–1307.*

[5] A.M. Cary, Jr., J.M. Hefner. 1970. Film cooling effectiveness in hypersonic turbulent flow. *AIAA Journal, Vol. 8, No. 11, Pp. 2090–2091.*

[6] Jerry N. Hefner, Aubrey M. Cary, Jr., Dennis M. Bushnell. Investigation of the three-dimensional turbulent flow downstream of swept slot injection in hypersonic flow. 1974. *AIAA Paper No. 74-679, ASME Paper No. 74-HT-13.*

[7] V. Zakkay, Chi R. Wang. 1973. Investigation of multiple slot film cooling to a blunt nose cone. *AIAA Paper No. 73-698.*

[8] A.J. Srokowski, F.G. Howard, M.V. Feller. 1976. Direct measurements at mach 6 of turbulent skin friction reduction by injection from single and multiple flush slots. *AIAA Paper No. 76-178.*

[9] V.Ya. Borovoy, Ed.B. Vasilevsky, I.V. Struminskaya, L.V. Yakovleva. 1998. Gas flow and heat protection by strong injection in the shock wave interference region near the blunt body front surface. *3rd European symposium on Aerothermodynamics for space vehicles, ESA SP-426 Proceedings.*

[10] J. Linn, M.J. Kloker. Numerical investigations of film cooling and its influence on the hypersonic boundary-layer flow. 2008. *Springer, RESPACE – Key Technologies for Reusable Space Systems, NNFM,* Vol. 98, *Pp. 151–169.*

[11] J. Linn, M. Keller, M.J. Kloker . Effects of inclined blowing on effusion cooling in a Mach-2.67 boundary layer. 2010. *Sonderforschungsbereich/Transregio 40 – Annual Report, Pp. 55–67.*

[12] J. Linn, M.J. Kloker. Effects of wall-temperature conditions on effusion cooling in a Mach-2.67 boundary layer. 2011. *AIAA Journal. Vol. 49, No. 2, Pp. 299–307.*

[13] M. Keller, M.J. Kloker . Numerical simulation of laminar film cooling in a supersonic boundary layer using modeled and simulated blowing. 2011. *Sonderforschungsbereich/Transregio 40 – Annual Report, Pp. 43–57.*

[14] M. Keller, M.J. Kloker. 2012. Influence of boundary-layer turbulence on effusion cooling at Mach 2.67. *Sonderforschungsbereich/Transreg io 40 – Annual Report, Pp. 1–13.*

[15] K.A. Heufer, H. Olivier. 2008 Experimental and numerical study of cooling gas injection in laminar supersonic flow. *AIAA Journal, Vol. 46, No. 11, Pp. 2741–2751.*

[16] M. Hombsch, H. Olivier. 2010. Flow condition and cooling gas variation for film cooling studies in hypersonic flow. *Sonderforschungsbereich/Transregio 40 – Annual Report, Pp. 27–39.*

[17] M. Hombsch, H. Olivier. Film cooling in turbulent supersonic flow. 2011. *Sonderforschungsbereich/Transregio 40 – Annual Report, Pp. 19–29.*

[18] V.Ya. Borovoy, A.Yu. Chinilov, V.N. Gusev, I.V. Struminskaya, J. Delery, B. Chanetz. 1997. Interference between a cylindrical bow shock and a plane oblique shock. *AIAA Journal, Vol. 35, No. 11, Pp. 1721–1728.*

[19] V. Mosharov, A. Orlov, V. Radchenko. 2003. Temperature sensitive paint (tsp) for heat transfer measurement in short duration wind tunnels. *20th ICIASF, Goettingen, Germany: Proc. CD.*

[20] V. Mosharov, V. Radchenko. 2007. Heat transfer measurements in short-duration wind tunnel by temperature sensitive paint. *TsAGI, Uchenye Zapiski, Vol. 38, No. 1.*

[21] Egorov I.V., Federov A.V., Soudakov V.G. 2006. Direct numerical simulation of disturbances generated by periodic suction-blowing in a hypersonic boundary layer. *Theor. Comput. Fluid Dyn., Vol. 20, No. 1, Pp. 41–54.*

[22] Bashkin V.A. 1964. Raschet koeffitsientov soprotivleniya treniya i teploperedachi plastiny, konusa i tuponosogo tela v okrestnosti kriticheskoy tochki pri laminarnom techenii v pogranichnom sloe bez ucheta dissotsiatsii. *Trudy TsAGI (rus), Materialy k raschetu soprotivleniya treniya i teploperedachi razlichnyh tel pri giperzvukovyh skorostyah, Vol. 937, Pp. 12–21.*

[23] Avduevsky V.S., Koshkin V.K. 1992. Osnovy teploperedachi v aviatsionnoy i raketno-kosmicheskoy tehnike. *Moskva: Mashinostroenie*.